



## HONO and its potential source particulate nitrite at an urban site in North China during the cold season



Liwei Wang<sup>a</sup>, Liang Wen<sup>a</sup>, Caihong Xu<sup>a</sup>, Jianmin Chen<sup>a,b</sup>, Xinfeng Wang<sup>a,\*</sup>, Lingxiao Yang<sup>a,b</sup>, Wenxing Wang<sup>a</sup>, Xue Yang<sup>a</sup>, Xiao Sui<sup>a</sup>, Lan Yao<sup>a</sup>, Qingzhu Zhang<sup>a</sup>

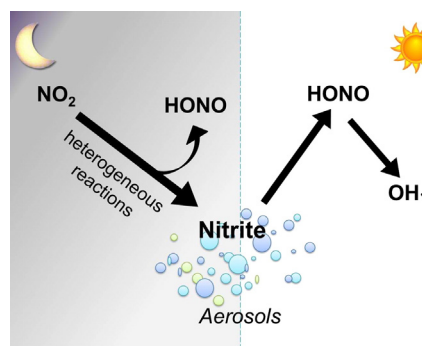
<sup>a</sup> Environment Research Institute, Shandong University, Ji'nan 250100, China

<sup>b</sup> School of Environmental Science and Engineering, Shandong University, Ji'nan 250100, China

### HIGHLIGHTS

- HONO and particulate nitrite were simultaneously measured in North China.
- Vehicle exhausts and NO<sub>2</sub> reactions are identified as major sources of HONO.
- Heterogeneous reactions of NO<sub>2</sub> produced a large amount of particulate nitrite.
- Particulate nitrite acted as a potential source of HONO especially in the daytime.

### GRAPHICAL ABSTRACT



### ARTICLE INFO

#### Article history:

Received 26 June 2015

Received in revised form 5 August 2015

Accepted 7 August 2015

Available online xxxx

Editor: D. Barcelo

#### Keywords:

HONO

Particulate nitrite

Source identification

Heterogeneous conversion

Transformation

### ABSTRACT

Characteristics and transformation of nitrous acid (HONO) and particulate nitrite were investigated with high time-resolution field measurements at an urban site in Ji'nan, China from Nov. 2013 to Jan. 2014. During the sampling period, averages of 0.35 ppbv HONO and 2.08  $\mu\text{g m}^{-3}$  fine particulate nitrite were observed. HONO and particulate nitrite exhibited similar diurnal variation patterns but differed in the time at which concentration peaks and valleys occurred. Elevated nocturnal HONO concentration peaks were mainly associated with primary emissions from vehicle exhaust and secondary formation via heterogeneous reactions of NO<sub>2</sub>. In fresh air masses dominated by vehicle emissions, the average HONO/NO<sub>x</sub> ratio was 0.58%. The nocturnal heterogeneous reactions of NO<sub>2</sub> contributed to about half of the elevated HONO concentration peaks, with the conversion rates in the range of 0.05% to 0.96% h<sup>-1</sup>. Meanwhile, a large amount of particulate nitrite, which greatly exceeded the concentration of the gas-phase HONO, was also produced through the heterogeneous reactions of NO<sub>2</sub>. The large yields of particulate nitrite were facilitated by abundant ammonia and particulate cations in urban Ji'nan. Notably, in the daytime, particulate nitrite acted as a potential source of HONO, especially in conditions of low humidity and acidic aerosols, which possibly has subsequent effects on photochemistry in the boundary layer.

© 2015 Elsevier B.V. All rights reserved.

\* Corresponding author.

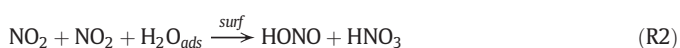
E-mail address: [xinfengwang@sdu.edu.cn](mailto:xinfengwang@sdu.edu.cn) (X. Wang).

## 1. Introduction

Nitrous acid (HONO) normally accumulates at nighttime and photo-dissociates during the daytime. The photolysis of HONO in the sunlight enhances the OH radicals (R1) present in the troposphere, especially in the early morning when other sources are weak (Zhou et al., 2001; Alicke et al., 2002; Acker et al., 2006; Kleffmann, 2007). In addition to the high levels of nocturnal HONO, a considerable amount of HONO is also frequently observed at daytime, suggesting the complexity of HONO sources and the existence of unknown ones (Kleffmann et al., 2003; Su et al., 2008a; Sörgel et al., 2011a; Li et al., 2012, 2014; Ma et al., 2013). Therefore, identification and evaluation of the various sources of HONO have become crucial to the recognition of current HONO chemistry (VandenBoer et al., 2014a).

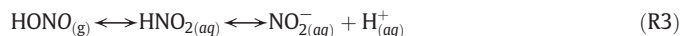


Ambient HONO originates not only from primary emission but also secondary formation. The predominant HONO source varies with locations and periods. In urban cities, a large fraction of HONO is emitted from vehicle exhaust especially during rush hours. In farmlands or forests, soil nitrite and bacteria act as an important emission sources (Su et al., 2011; Oswald et al., 2013). In most of other cases, however, chemical reactions of nitrogen oxides and/or other nitrogen-containing compounds produce more HONO. Among them, heterogeneous process of NO<sub>2</sub> on available surfaces is considered as the dominant formation pathway (R2). Both laboratory and field studies have reported that a significant amount of ambient HONO is converted from NO<sub>2</sub> on wet surfaces such as atmospheric aerosols (mineral dusts, soot, sulfates, organics, etc.), ground, plants, sea, and snow with different mechanisms and conversion rates (Zhou et al., 2001; Herrmann et al., 2010; Khalizov et al., 2010; Bedjanian and El Zein, 2012; Zha et al., 2014). The conversion coefficient mainly depends on the abundance of surface to volume ratios, the surface properties, and the ambient relative humidity (Finlayson-Pitts et al., 2003; Su et al., 2008b; Zha et al., 2014). Besides, other homogeneous and heterogeneous reactions and surface photolysis involving NO, NO<sub>2</sub>, and HNO<sub>3</sub> also contribute to the ambient HONO in some specific conditions (Li et al., 2012; Liu et al., 2014). Due to the various constituents of atmospheric trace pollutants and surfaces properties, researchers are far from having a full understanding of the sources of HONO, particularly in a polluted environment with intensive NO<sub>x</sub> emissions and high aerosol loading such as occurs in North China.



Particulate nitrite (NO<sub>2</sub><sup>-</sup>) has the same oxidation state of the nitrogen atom as HONO. Owing to its very low abundance and chemical instability (Lammel and Cape, 1996), little attention has been paid to particulate nitrite in past decades. In recent years, however, high levels of particulate nitrite in the troposphere have been observed, and it was revealed that particulate nitrite may serve as a potential reservoir of HONO (Song et al., 2009; VandenBoer et al., 2014b). The production of particulate nitrite from gas-phase HONO may occur on solution layers exposed to the atmosphere, such as wet aerosols, fog droplets, and surface water (Moore et al., 2004; He et al., 2006; Sörgel et al., 2011b; VandenBoer et al., 2014b). R3 demonstrates the reversible reaction and gas-aerosol partition between particulate nitrite and HONO, which depends on such factors as concentrations, acidity of the active surfaces, ambient temperature, and relative humidity. In acidic conditions, particulate nitrite reversibly associates with H<sup>+</sup> ions to yield HONO, such that high levels of particulate nitrite may also contribute to the sources of ambient HONO in the regions with severe particulate pollution. Therefore, recognition of particulate nitrite and its linkages to HONO is essential to provide complete insights into HONO chemistry

in such regions.



Ji'nan, the capital city of Shandong province, is located almost in the center of North China (a fast-growing region in past decades). The city has a temperate, semi-humid continental monsoon climate, which is rainless in spring, rainy and hot in summer, and dry and cold in autumn and winter. It covers an area of 8177.21 km<sup>2</sup> and has a population of approximately 7.0 million (SPBS, 2014). By the end of 2013, the number of vehicles in Ji'nan had surged to about 1.4 million, a rate of increase of about 14%. Due to the intensive emissions of air pollutants from vehicles and other sources such as industries, urban Ji'nan has been suffering from severe particulate matter pollution in the past decade, and elevated concentrations of particulate nitrite were observed there in our previous studies (e.g., Gao et al., 2011; Wang et al., 2012, 2014). In recent years, the city has devoted itself to reducing pollutant emissions by speeding up the elimination of “yellow label” vehicles and implementing stricter emission standards.

In this study, simultaneous on-line measurements of HONO and nitrite in PM<sub>2.5</sub> were made in urban Ji'nan during the cold season. Characteristics, sources, and transformation of HONO and particulate nitrite were analyzed in detail with the aid of related air pollutants, with the expectations of obtaining a comprehensive understanding of gas-phase HONO and particulate nitrite in the polluted urban boundary layer in North China and providing new insights into the chemistry of HONO.

## 2. Experiment and methods

### 2.1. Site description

Field measurements were conducted at the Atmospheric Environment Observation Station of Shandong University (AEOS-SDU) in urban Ji'nan (N36°40', E117°03'). It is located on the rooftop of a six-story teaching building on the central campus of the university, approximately 20 m above the ground. The inlets of the online instruments were installed about 1.5 m above the rooftop of the observation station. The sampling period lasted 41 days, from Nov. 26, 2013 to Jan. 5, 2014.

The AEOS-SDU site is surrounded by educational, residential, and commercial districts. It is located to the north of Shanda S Road and to the east of Shanda Road. Shanda N Road lies to the north, and Hongjialou S Road lies to the east (Fig. 1). There are several busy roads nearby: Jiefang Road (about 750 m to the south), Lishan Road (about 1200 m to the west), 2nd Ring Road E (about 1300 m to the east), and Huayuan Road (about 1100 m to the north). In addition to vehicle emissions, large-scale industries in suburban areas are important sources of emissions in Ji'nan. These industries are mainly distributed in the northeast (coal-combustion power plants, steel plant, and chemical plants) and southwest (cement plants).

### 2.2. Instruments

Data collected in this study included the concentrations of PM<sub>2.5</sub> water-soluble ions such as nitrite, nitrate, ammonia, and sulfate; PM<sub>2.5</sub> mass; trace gases of HONO, HNO<sub>3</sub>, NO<sub>x</sub>, and O<sub>3</sub>; and meteorological parameters. The involved monitors, analyzers, and sensors are described in detail below.

Water-soluble gases and ions in PM<sub>2.5</sub> were measured using the on-line Monitor for Aerosols and Gases in ambient air (MARGA, ADI20801, Applikon-ECN, Netherlands). A WRD (Wet Rotating Denuder) was used to capture the acidic and alkaline gases including HCl, HNO<sub>2</sub>, HNO<sub>3</sub>, and NH<sub>3</sub>, and a SJAC (Steam Jet Aerosol Collector) was equipped to collect the water-soluble ions in PM<sub>2.5</sub>. The sample solutions were then analyzed by two ion chromatographs (Makkonen et al., 2012; Khezri et al., 2013). Note that the measured data of HONO using the WRD

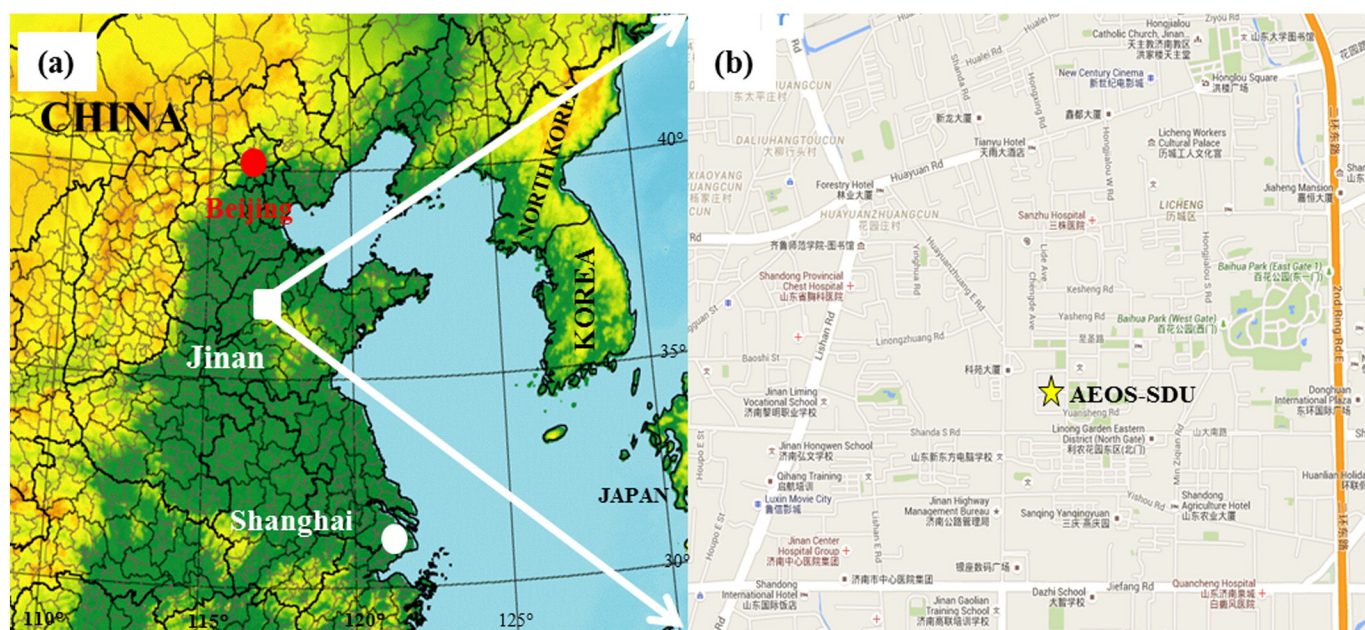


**Fig. 1.** (a) Topographic map of the study region which shows the locations of Ji'nan (marked in square) and some other major cities. (b) Specific location of the measurement site and roads nearby.

with absorption liquid of  $25 \text{ mg L}^{-1} \text{ Na}_2\text{CO}_3$  was previously discovered to be overestimated (Genfa et al., 2003). Therefore,  $15 \text{ ppmv H}_2\text{O}_2$  in water instead of  $\text{Na}_2\text{CO}_3$  was applied as absorption solution, which could efficiently oxidize S (IV) and avoid its reaction with  $\text{NO}_2$ . With the  $\text{H}_2\text{SO}_4$  formed, the absorption solution is acidified, and the heterogeneous reactions of  $\text{NO}_2$  in the WRD are impeded. Thus, any artifact present was the result of the conversion of  $\text{NO}_2$  on the surface of the sampling tube, and the overestimation was relatively small. Recent studies have also shown that the overestimation of HONO using WRD mainly occurs in the daytime (Khezri et al., 2013; Nie et al., 2015). Thus, we used only nocturnal HONO data except as described in Section 3.4. During the field study, LiBr solution ( $4.0 \text{ mg L}^{-1}$ ) was added to each sample as an internal standard. The aerosol and gas samples were collected by the MARGA at a flow rate of  $16.7 \text{ L min}^{-1}$  and analyzed at a time resolution of 1 h. During the collection period, 897 hourly samples were taken and analyzed.

$\text{PM}_{2.5}$  mass concentration was continuously measured by a Synchronized Hybrid Ambient Real-Time Particulate Monitor (SHARP Monitor, Model 5030; Thermo Fisher Scientific, USA) with a flow rate of  $16.7 \text{ L min}^{-1}$ . The absorption coefficient of beta rays and the scattering coefficient of 880 nm light were used to quantify the  $\text{PM}_{2.5}$  concentrations (Wen et al., 2015).

The concentrations of NO and  $\text{NO}_2$  were measured by chemiluminescence method (Model 42C, TEC, USA), which was equipped with a molybdenum oxide catalytic converter to convert  $\text{NO}_2$  into NO. An ultraviolet absorption method was applied to detect the  $\text{O}_3$  concentration (Model 49C, TEC, USA) (Wang et al., 2012; Wen et al., 2015). An automatic meteorological station (PC-4, JZYG, China) was used to collect meteorological data including temperature, relative humidity, and wind direction and speed. In the following analysis, 798 sets of hourly average data of these trace gases and meteorological parameters were collected and used.

### 3. Results and discussion

#### 3.1. General results of the observation

##### 3.1.1. Characteristics and concentrations

The average concentrations of HONO, NO,  $\text{NO}_2$ ,  $\text{O}_3$ ,  $\text{PM}_{2.5}$ , fine particulate nitrite and nitrate ( $\text{NO}_3^-$ ), and the ratios among them in urban Ji'nan

are listed in Table 1. During the measurement period, the average mixing ratios of HONO, NO,  $\text{NO}_2$ , and  $\text{O}_3$  were 0.35, 58.5, 46.9, and 16 ppbv, respectively. The average concentration of fine particulate nitrite was up to  $2.08 \mu\text{g m}^{-3}$ . The average molar or mass ratios of HONO/ $\text{NO}_x$ , HONO/ $\text{NO}_2$ ,  $\text{NO}_2^-/\text{NO}_2$ , and  $\text{NO}_3^-/\text{PM}_{2.5}$  were 0.006, 0.009, 0.021, and 0.17, respectively. The average HONO concentration observed in Ji'nan exceeded that measured at a background site in Hong Kong (0.126 ppbv, Zha et al., 2014), was comparable to that measured in urban Seoul (0.36 ppbv, Song et al., 2009), but was lower than those measured in most other megacities including Beijing (1.04 ppbv, Spataro et al., 2013), Shanghai (0.92 ppbv, Wang et al., 2013), Guangzhou (2.8 ppbv, Qin et al., 2009), and Santiago (1.5 ppbv, minimum of daily average, Elshorbany et al., 2009). Of note, the HONO concentration in Guangzhou (measured in the summer of 2006) exceeded that in Beijing (measured in the winter of 2006), probably due to the differences in emissions, season, and climate. Guangzhou has a subtropical monsoon climate (humid), whereas Beijing has a temperate monsoon climate. The HONO concentration in Shanghai (measured from 2010 to 2012) was lower than those in both Guangzhou and Beijing, partly because of the implementation of strict vehicle exhaust emission standards in recent years. Compared with that in other cities in China, the HONO concentration in Ji'nan in the cold season was very low,

**Table 1**

Statistics of major gaseous pollutants and water-soluble ions in  $\text{PM}_{2.5}$ .

Species	Concentration	Sampling instrument
$\text{PM}_{2.5}$ ( $\mu\text{g m}^{-3}$ )	$134.9 \pm 114.5$	SHARP
Nitrate ( $\mu\text{g m}^{-3}$ )	$23.43 \pm 19.93$	MARGA
Sulfate ( $\mu\text{g m}^{-3}$ )	$24.04 \pm 22.46$	MARGA
Nitrite ( $\mu\text{g m}^{-3}$ )	$2.08 \pm 2.31$	MARGA
HONO (ppbv)	$0.35 \pm 0.5$	MARGA
$\text{HNO}_3$ (ppbv)	$1.18 \pm 1.86$	MARGA
NO (ppbv)	$58.5 \pm 76.9$	42C
$\text{NO}_2$ (ppbv)	$46.9 \pm 21.7$	42C
$\text{NO}_x$ (ppbv)	$105.5 \pm 93.6$	42C
$\text{SO}_2$ (ppbv)	$43 \pm 33$	43C
$\text{O}_3$ (ppbv)	$16 \pm 13$	49C
HONO/NO	$0.0081 \pm 0.483$	
HONO/ $\text{NO}_x$	$0.0055 \pm 0.0149$	
HONO/ $\text{NO}_2$	$0.0093 \pm 0.018$	
$\text{NO}_2^-/\text{NO}_2$	$0.021 \pm 0.018$	
$\text{NO}_2^-/\sum \text{N(III)}$	$0.81 \pm 0.17$	
$\text{NO}_3^-/\text{PM}_{2.5}$	$0.17 \pm 0.07$	

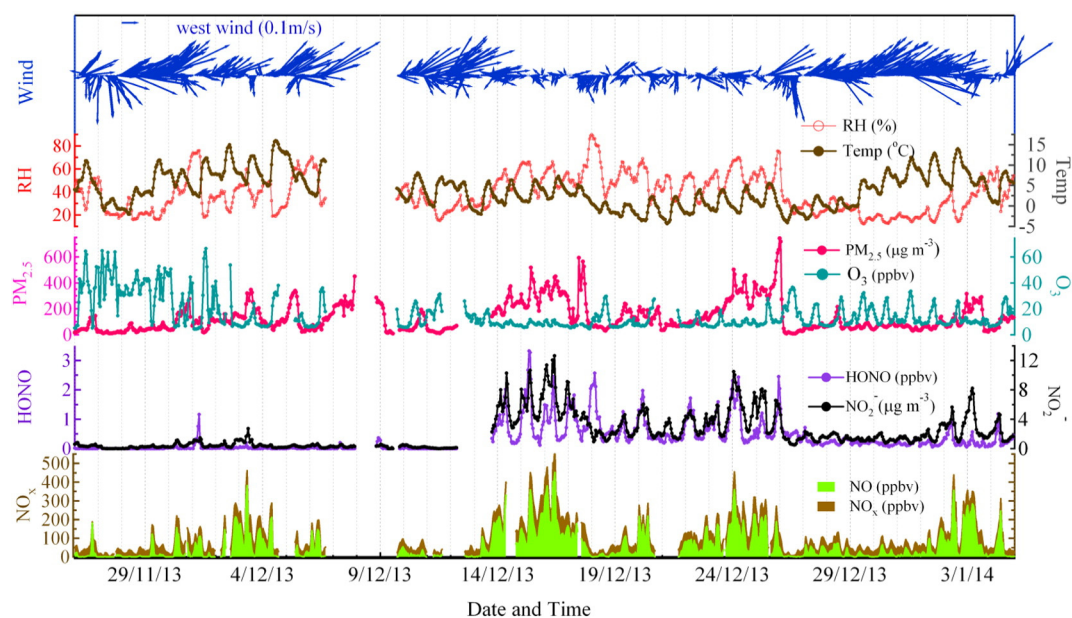


**Fig. 2.** Time series of concentrations of NO, NO<sub>2</sub>, HONO, O<sub>3</sub>, particulate nitrite, and PM<sub>2.5</sub>, and meteorological parameters of wind, temperature, and relative humidity during the sampling periods.

owing to the emissions, weather conditions, and the chemical processes occurring in this region, which are discussed in the following sections.

Despite the low concentrations of gas-phase HONO, a high level of fine particulate nitrite was observed in Ji'nan (2.08  $\mu\text{g m}^{-3}$  on average, with an average PM<sub>2.5</sub> concentration of 134.9  $\mu\text{g m}^{-3}$ ), which was much higher than those recorded in Bakersfield, California (0.15  $\mu\text{g m}^{-3}$ , VandenBoer et al., 2014a) and Beijing (0.12  $\mu\text{g m}^{-3}$ , Wang et al., 2005) and was comparable to the concentration in Seoul (1.41  $\mu\text{g m}^{-3}$ , Song et al., 2009). The average molar ratio of fine particulate nitrite to total nitrite (sum of HONO and fine particulate nitrite) was 0.81, and 97% of the NO<sub>2</sub><sup>-</sup> data exceeded the HONO concentrations. On average, approximately 1.37 ppbv (corresponding to 2.80  $\mu\text{g m}^{-3}$ ) of total nitrite was observed in urban Ji'nan, which is much higher than that in Gwangju (0.677 ppbv, Chang et al., 2008) and Seoul (1.05 ppbv, Song et al., 2009), indicating high levels of N (III) pollutants and possibly important roles of particulate nitrite in the atmospheric chemistry of this area.

Temporal variations of concentrations of aerosols and trace gases and meteorological parameters in Ji'nan are depicted in Fig. 2. Haze episodes occurred frequently, particularly from Dec. 13 to Dec. 26 when the wind speed was low and humidity was high. Throughout this period, high concentrations of HONO and particulate nitrite were observed along with high levels of NO<sub>x</sub> and PM<sub>2.5</sub>. The maximum hourly concentration of HONO was 3.39 ppbv, which occurred at 8:00 LT (local time) on Dec. 15, with simultaneous concentrations of NO, NO<sub>2</sub>, and PM<sub>2.5</sub> being 288.4 ppbv, 66.6 ppbv, and 270.0  $\mu\text{g m}^{-3}$ , respectively. The highest particulate nitrite concentration measured was 12.62  $\mu\text{g m}^{-3}$ , which occurred at 10:00 LT on Dec. 16, and simultaneously, concentrations of 452.8 ppbv for NO, 133.2 ppbv for NO<sub>2</sub> (the maximum value recorded during the measurement period), and 443.3  $\mu\text{g m}^{-3}$  for PM<sub>2.5</sub> were observed. The concurrent appearance of concentration peaks of these air pollutants suggests that high levels of HONO and particulate nitrite in urban Ji'nan are combined results of primary emissions, secondary formation via heterogeneous reactions of NO<sub>2</sub> on aerosol surfaces, and/or accumulation in adverse weather conditions. However, during the period from Nov. 27 to Dec. 12, very low concentrations of both HONO and nitrite were observed in conjunction with high levels of NO<sub>x</sub> and PM<sub>2.5</sub>. This was possibly associated with a special meteorological condition (e.g., high-speed wind from the southwest), intense solar radiation (as indicated by good visibility

and low humidity), and relatively high concentrations of atmospheric oxidants (e.g., ozone), which accelerated the oxidation of N (III).

### 3.1.2. Diurnal variation

Concentrations of HONO and particulate nitrite exhibited apparent diurnal variations (as shown in Fig. 3). From late afternoon, HONO concentrations started to increase and reached a peak (maximum average value of 0.58 ppbv) at 7:00 LT in the early morning. After sunrise, decomposition started in the presence of sunlight, and thus the concentration decreased to a minimum average of 0.16 ppbv at 13:00 LT in the early afternoon. Although the diurnal pattern of particulate nitrite was similar to that of HONO, the appearance of a concentration peak and valley occurred 1 or 2 h later than that of HONO. The maximum average concentration of particulate nitrite (3.00  $\mu\text{g m}^{-3}$ ) appeared at 8:00 LT, and the valley value was 1.17  $\mu\text{g m}^{-3}$  at 15:00 LT. These results indicate

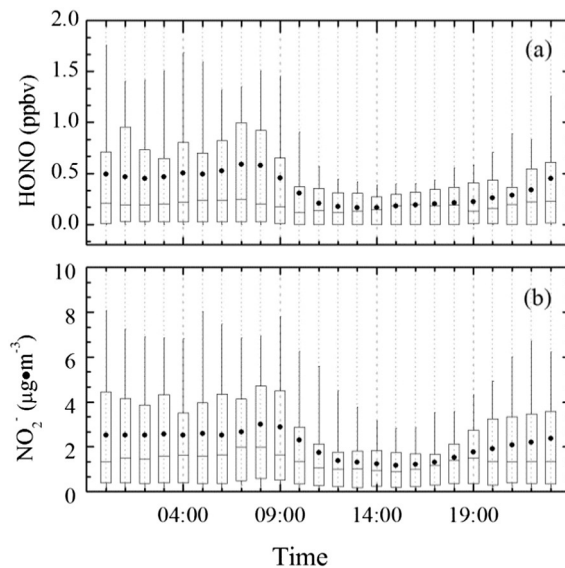


**Fig. 3.** Diurnal variations of (a) HONO and (b) fine particulate nitrite. The dot and the line in the boxes refer to the mean and median values, respectively. The boxes represent 50% (25% to 75%) and the lengths of whiskers donate 90% of the data.

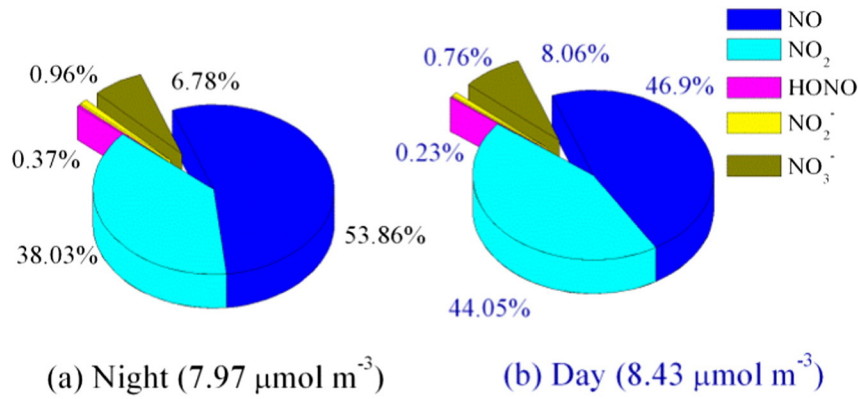


Fig. 4. Proportions of major nitrogen-containing components at (a) nighttime and (b) daytime (data of HNO<sub>3</sub> are not included because the concentrations were very low).

striking resemblances in sources and formation pathways between HONO and particulate nitrite, with the time lag attributable to the chemical transformation and equilibrium among them and related substances. The HONO concentration was the highest in autumn, followed by winter, summer, and spring in Beijing (Hendrick et al., 2014) and Hong Kong (Xu et al., 2015). The concentration of particulate nitrite in Ji'nan was high in winter and summer and relatively low in autumn and spring according to our previous study (Gao et al., 2011).

In general, the concentrations of HONO and particulate nitrite at nighttime were much higher than those at daytime. Moreover, the nocturnal proportions of HONO and nitrite in reactive nitrogen oxides were also higher than those during daytime: 0.37% and 0.96% versus 0.23% and 0.76% (Fig. 4). In contrast, the proportions of oxidized nitrogen-containing compounds such as NO<sub>2</sub> and particulate nitrate were remarkably higher at daytime than those at night, which was attributed to the strong oxidation capacity of photochemical oxidants in the presence of sunlight (Ma et al., 2013).

### 3.2. Direct emissions of HONO

To understand the contribution of direct emissions to the HONO concentration peaks, nocturnal HONO mixing ratios were analyzed in combination with wind directions and speeds. As shown in Fig. 5, elevated HONO concentrations (>0.5 ppbv) mostly occurred during periods of low wind speed (<1 m s<sup>-1</sup>). When the wind speed was above 1.5 m s<sup>-1</sup>, the HONO concentration was substantially below 0.3 ppbv. However, there was no significant linear correlation between the HONO concentration and wind speed. These results suggest that local emissions contribute significantly to the frequent nocturnal concentration peaks of HONO. The distribution characteristics of HONO with winds were quite similar to those of NO, with the majority of the increased concentrations emerging at low wind speeds (<1 m s<sup>-1</sup>) and lower concentrations emerging at high wind speeds, but were significantly different from those of NO<sub>2</sub> and SO<sub>2</sub>, indicating that traffic emissions had a strong influence on HONO peaks recorded at the sampling site.

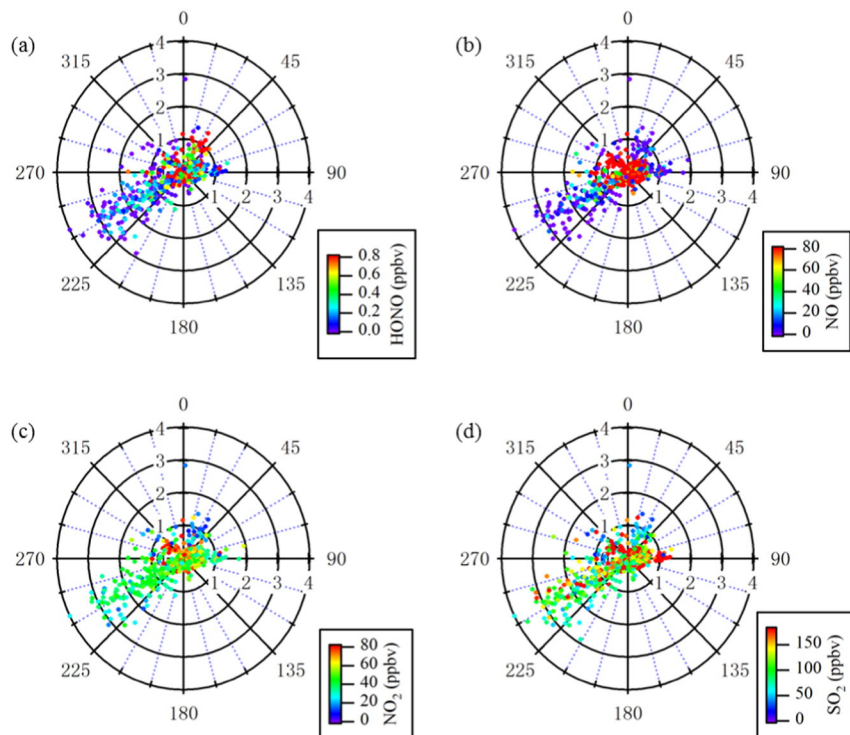


Fig. 5. Nighttime frequencies of wind directions and speeds for (a) HONO, (b) NO, (c) NO<sub>2</sub>, and (d) SO<sub>2</sub> during the measurement periods.

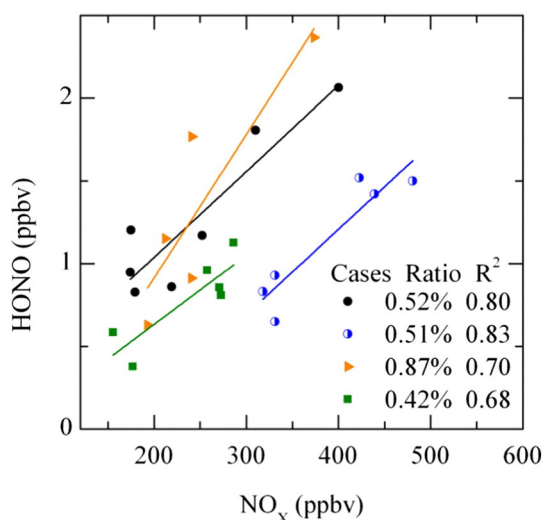


Fig. 6. Scatter plots of HONO and  $\text{NO}_x$  for four nocturnal cases.

The primary emission of HONO in urban Ji'nan is mainly attributed to vehicle exhaust. To further clarify the contributions of traffic emissions to the HONO concentration peaks, pollution cases were selected according to the following criteria: (a) only nocturnal data (to avoid the effects of photolysis in the daytime); (b)  $\text{NO}/\text{NO}_x$  ratio > 0.7; and (c)  $\text{NO} > 88$  ppbv (the highest 25% of  $\text{NO}$  data). Totally four cases were chosen here and analyzed in detail. As shown in Fig. 6, HONO correlated well with  $\text{NO}_x$  ( $0.68 \leq R^2 \leq 0.83$ ), with the HONO/ $\text{NO}_x$  ratio ranging from 0.42% to 0.87%. These results indicate that traffic emissions are a principal source of the HONO peaks. Under conditions dominated by traffic emissions, an average HONO/ $\text{NO}_x$  ratio of 0.58% was obtained at our sampling site. The ratios of HONO/ $\text{NO}_x$  have been reported to range from 0.3% to 0.8% in freshly emitted vehicle exhaust based on tunnel studies (e.g., Kleffmann et al., 2003; Kurtenbach et al., 2001). Therefore, 0.58% was reasonably chosen as the emission factor at this site and used to adjust the HONO data to exclude the contribution from traffic emissions in Section 3.3.

### 3.3. Heterogeneous formation of HONO and particulate nitrite

#### 3.3.1. Heterogeneous formation of HONO

Apart from direct emissions, a large fraction of HONO was produced from the heterogeneous reaction of  $\text{NO}_2$  on wet surfaces. To understand the contribution of the heterogeneous uptake of  $\text{NO}_2$  to the elevated HONO concentrations and the conversion efficiency, seven nighttime cases were selected and analyzed here. Instead of the original HONO concentration, an adjusted HONO concentration,  $\text{HONO}^*$ , was used to remove (or reduce) the influence from traffic emissions. The  $\text{HONO}^*$  concentration was calculated by subtracting the  $\text{NO}_x$  concentration timing factor of 0.58% obtained in the previous section (Eq. (1)). Considering all of the nocturnal data with HONO concentration peaks greater than 1 ppbv, approximately 42% of the HONO was contributed by traffic

emissions, and about half (~58%) was attributed to heterogeneous reactions of  $\text{NO}_2$ .

$$[\text{HONO}^*] = [\text{HONO}] - 0.58\% \times [\text{NO}] \quad (1)$$

Subsequently, the  $\text{NO}_2$ -to-HONO conversion efficiency was calculated following Eq. (2) (Alicke et al., 2002; Li et al., 2012).

$$C_{\text{HONO}} = \frac{[\text{HONO}^*]_{t_2} - [\text{HONO}^*]_{t_1}}{[\overline{\text{NO}_2}] \times (t_2 - t_1)} \quad (2)$$

Here,  $[\overline{\text{NO}_2}]$  represents the average  $\text{NO}_2$  concentration over the time interval  $t_1$  to  $t_2$ .

$C_{\text{HONO}}$  and HONO mixing ratios in these cases are summarized in Table 2. The adjusted HONO concentrations showed large variability (less than 0.1 to 2.5 ppbv). As depicted,  $\text{HONO}^*$  concentrations correlated well with the  $\text{NO}_2$  mixing ratios in most cases ( $0.54 \leq R^2 \leq 0.89$ ), suggesting that the heterogeneous reactions of  $\text{NO}_2$  were the major formation pathways of the enhanced HONO during these periods. Similar to  $\text{HONO}^*$ ,  $C_{\text{HONO}}$  also showed great variability, from 0.05% to 0.96%  $\text{h}^{-1}$  with an average of 0.29%  $\text{h}^{-1}$ . The conversion efficiency in urban Ji'nan was lower than those observed in Guangzhou (1.6%  $\text{h}^{-1}$ , Su et al., 2008a; Li et al., 2012), Shanghai (0.7%  $\text{h}^{-1}$ , Wang et al., 2013), and Hong Kong (0.52%  $\text{h}^{-1}$ , Xu et al., 2015). Apart from case 3 on Dec. 17, the  $C_{\text{HONO}}$  values correlated well with  $\text{PM}_{2.5}$  ( $R^2 = 0.84$ ), suggesting that the aerosol surface is of vital importance to the  $\text{NO}_2$ -to-HONO conversion efficiency under severe haze conditions. In addition, very good correlation was found between relative humidity and  $\text{NO}_2$ -to-HONO conversion efficiency ( $R^2 = 0.92$ ). It is possible that the conversion rate is strongly influenced by the liquid water content, which correlates positively with relative humidity.

#### 3.3.2. Heterogeneous formation of particulate nitrite

Besides HONO, particulate nitrite is another important product of the heterogeneous reactions of  $\text{NO}_2$  in the troposphere. Moderately good correlations were found between nocturnal nitrite and  $\text{NO}_2$  (see Fig. 7). In conditions of moderate and high humidity ( $\text{RH} > 50\%$ ), the concentration of particulate nitrite increased as the concentration of  $\text{NO}_2$  rose with an average slope of 0.10 ( $\mu\text{g m}^{-3}$  ppbv $^{-1}$ ), indicating the formation of particulate nitrite from the heterogeneous reaction of  $\text{NO}_2$ . When the relative humidity was low (<50%), the level of particulate nitrite was relatively low and changed little with  $\text{NO}_2$  concentration in that the heterogeneous reactions of  $\text{NO}_2$  were inhibited.

Six nocturnal cases were further analyzed to explore the formation of elevated concentrations of particulate nitrite (Fig. 8). These cases lasted from 6 to 14 h, during which the concentration of nitrite rose positively with  $\text{NO}_2$  concentration. Strong correlations ( $0.68 \leq R^2 \leq 0.92$ ) between the concentrations indicated that the heterogeneous process is one of the major formation pathways of particulate nitrite and makes a significant contribution to the elevated concentrations of nocturnal particulate nitrite during the cold season in urban areas of Ji'nan. In the six pollution cases, the slope of fine  $\text{NO}_2^-$  versus  $\text{NO}_2$  ranged from 0.045 to 0.250 ( $\mu\text{g m}^{-3}$  ppbv $^{-1}$ ), with the maximum slope of 0.250 occurring during the night of Dec. 15.

Table 2  
 $C_{\text{HONO}}$ ,  $R^2$  and other supportive information for seven nocturnal cases.

Case	Date	Time	$R^2$	$C_{\text{HONO}}$ (% $\text{h}^{-1}$ )	$\text{HONO}^*$ (ppbv)	$\text{RH}^a$ (%)	$\text{PM}_{2.5}^a$ ( $\mu\text{g m}^{-3}$ )
1	Dec. 15, 2013	01:00–07:00	0.58	0.34	0.88–1.53	65	227.4
2	Dec. 17, 2013	00:00–05:00	0.52	0.13	0.45–0.82	51	162.9
3	Dec. 17, 2013	19:00–03:00	0.90	0.96	0.41–2.50	81	91.3
4	Dec. 18, 2013	19:00–22:00	0.90	0.10	0.26–0.39	48	69.1
5	Dec. 19, 2013	19:00–23:00	0.82	0.05	0.29–0.43	51	124.1
6	Dec. 24, 2013	03:00–07:00	0.92	0.42	0.20–1.10	69	342.5
7	Jan. 04, 2014	19:00–23:00	0.93	0.12	0.11–0.29	50	144.3

<sup>a</sup> Mean value of the selected case period.

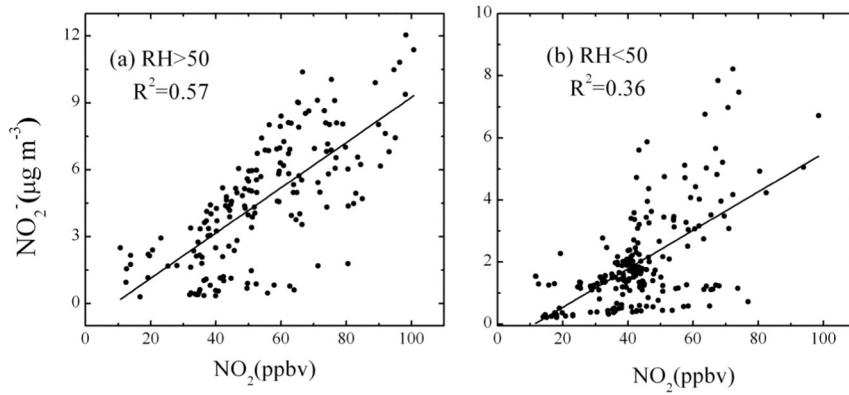


Fig. 7. Scatter plots of fine particulate nitrite versus  $\text{NO}_2$  with (a)  $\text{RH} > 50\%$  and (b)  $\text{RH} < 50\%$ .

Generally, the  $\text{NO}_2$ -to-nitrite conversion efficiency is promoted with a larger active water layer surface (e.g., higher relative humidity and  $\text{PM}_{2.5}$  mass concentration), favorable surface chemical environment (e.g., alkaline aerosols and less oxidants), and steady meteorological conditions. On Dec. 15, high relative humidity (65% on average), elevated  $\text{PM}_{2.5}$  mass concentration, sufficient ammonium cations, low levels of ozone, and low wind speeds all facilitated the heterogeneous reactions and led to an extremely high conversion efficiency.

The high ratios of particulate nitrite to total nitrites and the good correlations between particulate nitrite and  $\text{NO}_2$  suggest that a large fraction of heterogeneous products is presented in particulate form instead of gas-phase HONO. Here, the concentration of free cation (equivalent concentration) was calculated to evaluate the existence of nitrite with consideration of all of the major ions in fine particles (Eq. (3)).

$$\text{Cation}_{(p, \text{free})} = \left( \text{NH}_4^+_{(p)} + \text{Na}^+_{(p)} + \text{K}^+_{(p)} + \left( 2 \times \text{Ca}^{2+}_{(p)} \right) + \left( 2 \times \text{Mg}^{2+}_{(p)} \right) \right) - \left( \left( 2 \times \text{SO}_4^{2-}_{(p)} \right) + \text{NO}_3^-_{(p)} + \text{Cl}^-_{(p)} \right) \quad (3)$$

It is worth noting that ammonium contributed the most among the five major cations and was produced from the rich ammonia ( $9.1 \pm 6.3$  ppbv on average) present in urban Ji'nan.

Throughout the nocturnal elevations, the majority of the free cation concentrations were higher than the peak concentrations of particulate nitrite, i.e., the cations were in excess. Good correlation ( $R^2 = 0.68$ ) was found between them, and particulate nitrite concentrations increased positively with the free cations in most of the periods. Therefore, the formation of particulate nitrite in urban Ji'nan is enhanced by the presence of rich ammonia, and there are abundant cations left to neutralize the newly produced nitrite in wet aerosols or small droplets. As a result, particulate nitrite became the dominant product of the heterogeneous processes of  $\text{NO}_2$ , and the nocturnal HONO presented relatively low concentration in North China during the cold season.

#### 3.4. Release of HONO from particulate nitrite during the daytime

Gas-phase HONO could be produced from high levels of particulate nitrite in suitable conditions. The release of HONO from particulate nitrite is promoted when the ambient temperature is high, humidity is low, and in particular, the aerosols are acidic.

Neutralization degree ( $F$ ) is used here to represent the acidity of the aerosols and is calculated using the equivalent concentrations of the major ions: sulfate, nitrate, and ammonium (Eq. (4)) (Zhou et al., 2012).

$$F = [\text{NH}_4^+] / \left( 2 \times [\text{SO}_4^{2-}] + [\text{NO}_3^-] \right) \quad (4)$$

As illustrated in Fig. 9, gas-phase HONO formation was observed in urban Ji'nan with the concurrent decrease in particulate nitrite concentration in the daytime. From the late morning to the early afternoon (11:00–15:00 LT) on Dec. 18, there was a sharp decrease in the relative humidity (from 52% to 35%), leading to a very dry environment (little liquid water available on aerosol surfaces). Moreover, the aerosols were slightly acidic ( $F$  value  $< 1$  at most times during the period). The HONO concentration exhibited a continuous increase from 0.25 to 0.53 ppbv. Within the 4 h, the concentration of fine nitrite decreased from 2.00 to 1.04  $\mu\text{g m}^{-3}$ . The ratio of fine particulate nitrite to the total nitrites also decreased from 0.77 to 0.50. The rate of decrease in particulate nitrite concentration was approximately  $0.24 \mu\text{g m}^{-3} \text{h}^{-1}$ . Simultaneously, the rate of increase of the HONO concentration was  $0.06 \text{ ppbv} \cdot \text{h}^{-1}$  ( $\sim 0.13 \mu\text{g m}^{-3} \text{h}^{-1}$ ), suggesting the release of HONO from nitrite. On Dec. 26, from 10:00 LT in the morning to 15:00 LT in the afternoon, the relative humidity was very low (ranging from 22% to 30%), and the aerosols were acidic with the  $F$  value decreased to  $\sim 0.8$ . During this period, although the particulate nitrite concentration was low (substantially below  $0.90 \mu\text{g m}^{-3}$ ), a significant increase in the HONO concentration (from 0.39 to 0.60 ppbv) was observed with a simultaneous decline in the fine nitrite concentration. The average rate of increase of the HONO concentration was  $0.03 \text{ ppbv} \cdot \text{h}^{-1}$  ( $\sim 0.06 \mu\text{g m}^{-3} \text{h}^{-1}$ ), and the rate of decrease of the fine nitrite was  $0.08 \mu\text{g m}^{-3} \text{h}^{-1}$  – close to the rate of increase of the HONO. In this case, the proportion of fine particulate nitrite in total nitrites decreased from 0.52 to 0.30, i.e., almost half of the fine particulate nitrite was converted into gas-phase HONO. Moreover, the  $\text{NO}_x$  concentrations during these two periods were substantially low (less than 15 and 9 ppbv, respectively), indicating limited contributions to HONO from other sources such as traffic emissions and heterogeneous reactions of  $\text{NO}_2$ .

It is well known that photolysis of HONO is an important source of OH radicals in the daytime. The high levels of particulate nitrite in

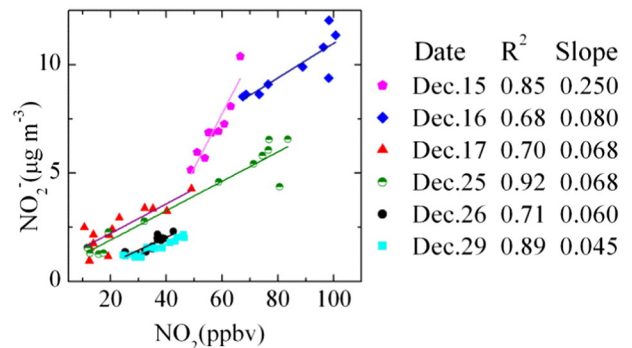
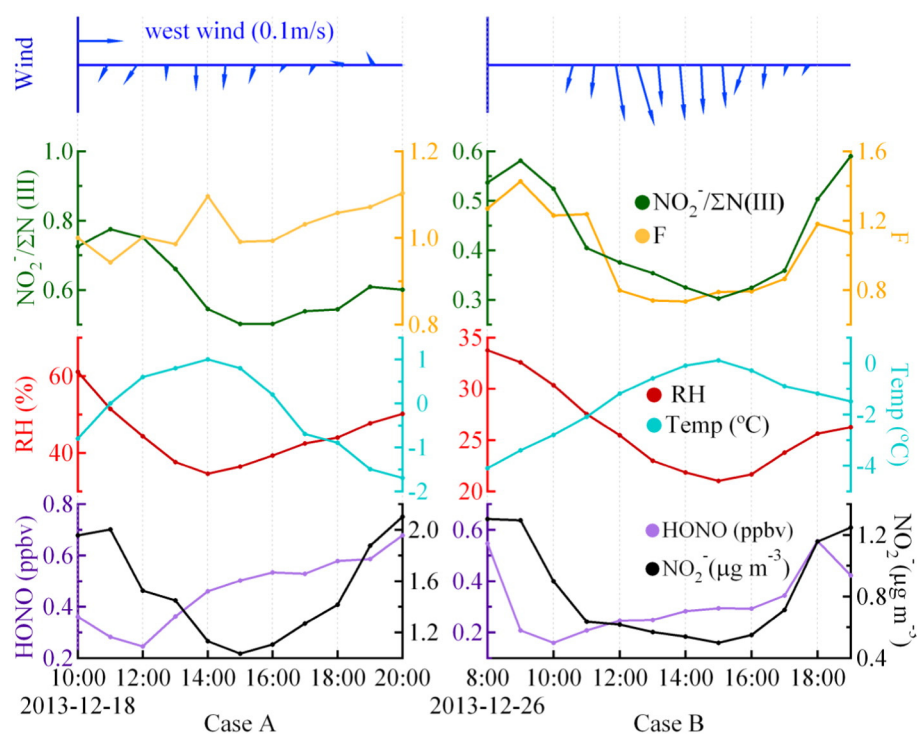


Fig. 8. Correlations between fine particulate nitrite and  $\text{NO}_2$  for six nocturnal cases.



**Fig. 9.** Temporal variations of HONO, fine particulate nitrite, ambient temperature, RH,  $\text{NO}_2/\Sigma\text{N(III)}$  ratio and  $F$  value for two selected cases. Case A lasted from 10:00 to 20:00 LT on Dec. 18 and case B started on 8:00 LT and ended at 19:00 LT on Dec. 26. The  $\text{NO}_2$  ratio and  $F$  value were estimated based on the measured data (see main text).

urban Ji'nan and the enhanced aerosol-gas conversion in conditions of low humidity and acidic aerosols made the particulate nitrite an important source of HONO, especially during the daytime, and produced subsequent effects on the photochemistry in the boundary layer.

#### 4. Summary and conclusions

High time-resolution field measurements of HONO, particulate nitrite in  $\text{PM}_{2.5}$ , related air pollutants, and meteorological parameters were conducted in urban Ji'nan in North China from Nov. 26, 2013 to Jan. 4, 2014. During the measurement period, the mean concentrations of HONO and fine particulate nitrite were 0.35 ppbv and  $2.08 \mu\text{g m}^{-3}$ , with the maximum hourly concentrations recorded of 3.39 ppbv and  $12.62 \mu\text{g m}^{-3}$ , respectively. The concentrations of both HONO and fine particulate nitrite exhibited distinct diurnal cycles with peaks in the early morning and valleys in the early afternoon. Elevated nocturnal HONO concentration peaks were associated with primary emissions from vehicle exhaust and secondary formation via heterogeneous reactions of  $\text{NO}_2$ . The average  $\text{HONO}/\text{NO}_x$  ratio during the periods with fresh vehicle emissions was 0.58%. The efficiency of the heterogeneous conversion of  $\text{NO}_2$  to HONO, ranging from 0.05% to  $0.96 \text{ h}^{-1}$ , strongly depended on the humidity and the aerosol loading. Overall, secondary formation contributed to about half of the elevated HONO concentration peaks. In addition, the heterogeneous reactions of  $\text{NO}_2$  on aerosol surfaces also produced significant amounts of particulate nitrite. Abundant ammonia and alkaline substance in fine particles enhanced the heterogeneous formation of particulate nitrite and thus made it the major product instead of gas-phase HONO in urban Ji'nan. However, during the daytime, particulate nitrite acted as a potential source of HONO. Gas-phase HONO was released especially in conditions of low humidity and acidic aerosols. The enhanced aerosol-gas conversion and high levels of particulate nitrites make non-negligible contributions to the production of HONO and thus have subsequent effects on the photochemistry in the boundary layer in North China. With the implementation of stricter vehicle emission standards in China, the emissions and productions of HONO and

particulate nitrite are expected to decrease in the future. However, the concurrent control of ammonia emissions may lead to enhanced release of gas-phase HONO from particulate nitrite in the acid aerosol condition.

#### Acknowledgments

This work was supported by Taishan Scholar Grand (ts20120552), National Natural Science Foundation of China (Nos. 41275123, 41375126, 21407094, 21307074), Natural Science Foundation of Shandong Province (No. ZR2014BQ031), and Strategic Priority Research Program of the Chinese Academy of Sciences (No. XDB05010200).

#### References

- Acker, K., Möller, D., Wiprecht, W., Meixner, F.X., Bohn, B., Gilge, S., et al., 2006. Strong daytime production of OH from  $\text{HNO}_2$  at a rural mountain site. *Geophys. Res. Lett.* 33.
- Alicke, B., Platt, U., Stutz, J., 2002. Impact of nitrous acid photolysis on the total hydroxyl radical budget during the Limitation of Oxidant Production/Pianura Padana Produzione di Ozono study in Milan. *J. Geophys. Res.* 107.
- Bedjanian, Y., El Zein, A., 2012. Interaction of  $\text{NO}_2$  with  $\text{TiO}_2$  surface under UV irradiation: products study. *J. Phys. Chem. A* 116, 1758–1764.
- Chang, W., Choi, J., Hong, S., Lee, J.H., 2008. Simultaneous measurements of gaseous nitrous acid and particulate nitrite using diffusion scrubber/steam chamber/luminol chemiluminescence. *Bull. Kor. Chem. Soc.* 29, 1525–1532.
- Elsorbany, Y., Kurtenbach, R., Wiesen, P., Lissi, E., Rubio, M., Villena, G., et al., 2009. Oxidation capacity of the city air of Santiago, Chile. *Atmos. Chem. Phys.* 9, 2257–2273.
- Finlayson-Pitts, B.J., Wingen, L.M., Sumner, A.L., Syomin, D., Ramazan, K.A., 2003. The heterogeneous hydrolysis of  $\text{NO}_2$  in laboratory systems and in outdoor and indoor atmospheres: an integrated mechanism. *Phys. Chem. Chem. Phys.* 5, 223–242.
- Gao, X., Yang, L., Cheng, S., Gao, R., Zhou, Y., Xue, L., et al., 2011. Semi-continuous measurement of water-soluble ions in  $\text{PM}_{2.5}$  in Jinan, China: temporal variations and source apportionments. *Atmos. Environ.* 45, 6048–6056.
- Genfa, Z., Slanina, S., Boring, C.B., Jongejan, P.A., Dasgupta, P.K., 2003. Continuous wet denuder measurements of atmospheric nitric and nitrous acids during the 1999 Atlanta Supersite. *Atmos. Environ.* 37, 1351–1364.
- He, Y., Zhou, X., Hou, J., Gao, H., Bertman, S.B., 2006. Importance of dew in controlling the air – surface exchange of HONO in rural forested environments. *Geophys. Res. Lett.* 33.
- Hendrick, F., Müller, J.F., Clémer, K., Wang, P., De Mazière, M., Fayt, C., et al., 2014. Four years of ground-based MAX-DOAS observations of HONO and  $\text{NO}_2$  in the Beijing area. *Atmos. Chem. Phys.* 14, 765–781.

- Herrmann, H., Hoffmann, D., Schaefer, T., Brüner, P., Tilgner, A., 2010. Tropospheric aqueous-phase free-radical chemistry: radical sources, spectra, reaction kinetics and prediction tools. *ChemPhysChem* 11, 3796–3822.
- Khalizov, A.F., Cruz-Quinones, M., Zhang, R., 2010. Heterogeneous reaction of NO<sub>2</sub> on fresh and coated soot surfaces. *J. Phys. Chem. A* 114, 7516–7524.
- Khezri, B., Mo, H., Yan, Z., Chong, S.-L., Heng, A.K., Webster, R.D., 2013. Simultaneous on-line monitoring of inorganic compounds in aerosols and gases in an industrialized area. *Atmos. Environ.* 80, 352–360.
- Kleffmann, J., 2007. Daytime sources of nitrous acid (HONO) in the atmospheric boundary layer. *ChemPhysChem* 8, 1137–1144.
- Kleffmann, J., Kurtenbach, R., Lörzer, J., Wiesen, P., Kalthoff, N., Vogel, B., et al., 2003. Measured and simulated vertical profiles of nitrous acid—part I: field measurements. *Atmos. Environ.* 37, 2949–2955.
- Kurtenbach, R., Becker, K.H., Gomes, J.A.G., Kleffmann, J., Lörzer, J.C., Spittler, M., et al., 2001. Investigations of emissions and heterogeneous formation of HONO in a road traffic tunnel. *Atmos. Environ.* 35, 3385–3394.
- Lammel, G., Cape, J.N., 1996. Nitrous acid and nitrite in the atmosphere. *Chem. Soc. Rev.* 25, 361–369.
- Li, X., Brauers, T., Häsel, R., Bohn, B., Fuchs, H., Hofzumahaus, A., et al., 2012. Exploring the atmospheric chemistry of nitrous acid (HONO) at a rural site in Southern China. *Atmos. Chem. Phys.* 12, 1497–1513.
- Li, X., Rohrer, F., Hofzumahaus, A., Brauers, T., Haeseler, R., Bohn, B., et al., 2014. Missing gas-phase source of HONO inferred from Zeppelin measurements in the troposphere. *Science* 344, 292–296.
- Liu, Z., Wang, Y., Costabile, F., Amoroso, A., Zhao, C., Huey, L.G., et al., 2014. Evidence of aerosols as a media for rapid daytime HONO production over China. *Environ. Sci. Technol.* 48, 14386–14391.
- Ma, J., Liu, Y., Han, C., Ma, Q., Liu, C., He, H., 2013. Review of heterogeneous photochemical reactions of NO<sub>y</sub> on aerosol – a possible daytime source of nitrous acid (HONO) in the atmosphere. *J. Environ. Sci.* 25, 326–334.
- Makkonen, U., Virkkula, A., Mäntykenttä, J., Hakola, H., Keronen, P., Vakkari, V., et al., 2012. Semi-continuous gas and inorganic aerosol measurements at a Finnish urban site: comparisons with filters, nitrogen in aerosol and gas phases, and aerosol acidity. *Atmos. Chem. Phys.* 12, 5617–5631.
- Moore, K.F., Eli Sherman, D., Reilly, J.E., Hannigan, M.P., Lee, T., Collett Jr., J.L., 2004. Drop size-dependent chemical composition of clouds and fogs. Part II: relevance to interpreting the aerosol/trace gas/fog system. *Atmos. Environ.* 38, 1403–1415.
- Nie, W., Ding, A.J., Xie, Y.N., Xu, Z., Mao, H., Kerminen, V.M., et al., 2015. Influence of biomass burning plumes on HONO chemistry in eastern China. *Atmos. Chem. Phys.* 15, 1147–1159.
- Oswald, R., Behrendt, T., Ermel, M., Wu, D., Su, H., Cheng, Y., et al., 2013. HONO emissions from soil bacteria as a major source of atmospheric reactive nitrogen. *Science* 341, 1233–1235.
- Qin, M., Xie, P., Su, H., Gu, J., Peng, F., Li, S., et al., 2009. An observational study of the HONO–NO<sub>2</sub> coupling at an urban site in Guangzhou City, South China. *Atmos. Environ.* 43, 5731–5742.
- Song, C.H., Park, M.E., Lee, E.J., Lee, J.H., Lee, B.K., Lee, D.S., et al., 2009. Possible particulate nitrite formation and its atmospheric implications inferred from the observations in Seoul, Korea. *Atmos. Environ.* 43, 2168–2173.
- Sörgel, M., Regelin, E., Bozem, H., Diesch, J.-M., Drewnick, F., Fischer, H., et al., 2011a. Quantification of the unknown HONO daytime source and its relation to NO<sub>2</sub>. *Atmos. Chem. Phys.* 11, 10433–10447.
- Sörgel, M., Trebs, I., Serafimovich, A., Moravek, A., Held, A., Zetzsch, C., 2011b. Simultaneous HONO measurements in and above a forest canopy: influence of turbulent exchange on mixing ratio differences. *Atmos. Chem. Phys.* 11, 841–855.
- Spataro, F., Ianniello, A., Esposito, G., Allegrini, L., Zhu, T., Hu, M., 2013. Occurrence of atmospheric nitrous acid in the urban area of Beijing (China). *Sci. Total Environ.* 447, 210–224.
- SPBS (Shandong Provincial Bureau of Statistics), 2014. Shandong Statistical Yearbook 2014. China Statistics Press, Beijing (Available online at <http://www.stats-sd.gov.cn/tjnj/nj2014/indexch.htm>).
- Su, H., Cheng, Y.F., Shao, M., Gao, D.F., Yu, Z.Y., Zeng, L.M., et al., 2008a. Nitrous acid (HONO) and its daytime sources at a rural site during the 2004 PRIDE-PRD experiment in China. *J. Geophys. Res.* 113, D14312.
- Su, H., Cheng, Y.F., Cheng, P., Zhang, Y.H., Dong, S., Zeng, L.M., et al., 2008b. Observation of nighttime nitrous acid (HONO) formation at a non-urban site during PRIDE-PRD2004 in China. *Atmos. Environ.* 42, 6219–6232.
- Su, H., Cheng, Y.F., Oswald, R., Behrendt, T., Trebs, I., Meixner, F.X., et al., 2011. Soil nitrite as a source of atmospheric HONO and OH radicals. *Science* 333, 1616–1618.
- VandenBoer, T.C., Young, C.J., Talukdar, R.K., Markovic, M.Z., Brown, S.S., Roberts, J.M., et al., 2014a. Nocturnal loss and daytime source of nitrous acid through reactive uptake and displacement. *Nat. Geosci.* 8, 55–60.
- VandenBoer, T.C., Markovic, M.Z., Sanders, J.E., Ren, X., Pusede, S.E., Browne, E.C., et al., 2014b. Evidence for a nitrous acid (HONO) reservoir at the ground surface in Bakersfield, CA, during CalNex 2010. *J. Geophys. Res.* 119, 9093–9106.
- Wang, Y., Zhuang, G., Tang, A., Yuan, H., Sun, Y., Chen, S., et al., 2005. The ion chemistry and the source of PM<sub>2.5</sub> aerosol in Beijing. *Atmos. Environ.* 39, 3771–3784.
- Wang, X., Wang, W., Yang, L., Gao, X., Nie, W., Yu, Y., et al., 2012. The secondary formation of inorganic aerosols in the droplet mode through heterogeneous aqueous reactions under haze conditions. *Atmos. Environ.* 63, 68–76.
- Wang, S., Zhou, R., Zhao, H., Wang, Z., Chen, L., Zhou, B., 2013. Long-term observation of atmospheric nitrous acid (HONO) and its implication to local NO<sub>2</sub> levels in Shanghai, China. *Atmos. Environ.* 77, 718–724.
- Wang, X., Chen, J., Sun, J., Li, W., Yang, L., Wen, L., et al., 2014. Severe haze episodes and seriously polluted fog water in Ji'nan, China. *Sci. Total Environ.* 493, 133–137.
- Wen, L., Chen, J., Yang, L., Wang, X., Caihong, X., Sui, X., et al., 2015. Enhanced formation of fine particulate nitrate at a rural site on the North China Plain in summer: the important roles of ammonia and ozone. *Atmos. Environ.* 101, 294–302.
- Xu, Z., Wang, T., Wu, J., Xue, L., Chan, J., Zha, Q., et al., 2015. Nitrous acid (HONO) in a polluted subtropical atmosphere: seasonal variability, direct vehicle emissions and heterogeneous production at ground surface. *Atmos. Environ.* 106, 100–109.
- Zha, Q., Xue, L., Wang, T., Xu, Z., Yeung, C., Louie, P.K.K., et al., 2014. Large conversion rates of NO<sub>2</sub> to HNO<sub>2</sub> observed in air masses from the South China Sea: evidence of strong production at sea surface? *Geophys. Res. Lett.* 41, 7710–7715.
- Zhou, X., Beine, H.J., Honrath, R.E., Fuentes, J.D., Simpson, W., Shepson, P.B., et al., 2001. Snowpack photochemical production of HONO: a major source of OH in the Arctic boundary layer in springtime. *Geophys. Res. Lett.* 28, 4087–4090.
- Zhou, Y., Xue, L., Wang, T., Gao, X., Wang, Z., Wang, X., et al., 2012. Characterization of aerosol acidity at a high mountain site in central eastern China. *Atmos. Environ.* 51, 11–20.